

# Reduction of Cogging Torque Technique in Sequential of Permanent Magnet Flux Switching Motor

Noor Faradilah Afiqah Hasan<sup>1</sup>, Erwan Sulaiman<sup>1, \*</sup>

<sup>1</sup>Faculty of Electrical and Electronic Engineering,  
Universiti Tun Hussein Onn, Batu Pahat, 86400, MALAYSIA

\*Corresponding Author Designation

DOI: <https://doi.org/10.30880/eeee.2022.03.01.009>

Received 05 February 2022; Accepted 27 March 2022; Available online 30 June 2022

**Abstract:** A study of several electric motors has been conducted on permanent magnet flux switching motors because it shows an excellent performance such as higher torque density, high efficiency, low vibration, and ease to control. However, this motor design encountered high cogging torque due to the interchange of permanent magnets in stator and rotor teeth. This study aims to improve the cogging torque of single-phase 4S-8P PM-FSM by implementing a reduction cogging torque technique in sequential. The initial design of 4S/8P PM-FSM is analyzed using JMAG Designer software. Three classical cogging torque reduction techniques will be applied to the motor notching, chamfering, and pole-pairing. These three classical cogging torque techniques will be tested individually, and the lowest cogging torque produced in each result will be selected for the next sequential. The performance of cogging torque is minimized from an initial value of as much as 35% from the initial design, which is from 1.7722 Nm to 1.1116 Nm.

**Keywords:** Cogging Torque, PM-FSM, Notching, Pole Pairing, Chamfering

## 1. Introduction

One of the new types of permanent magnet motor is flux switching motor (FSM). A permanent magnet flux switching engine (PM-FSM) shows an excellent performance with higher torque density, high power, and high flux-weakening capability compared to another conventional permanent magnet [1]. The PM-FSM is introduced by using a salient dual structure in both stator and rotor, where the armature coil and permanent magnet are located in the stator and a core in the rotor [2]. The operating principle of PM-FSM is based on armature flux linkage interaction with switching flux in positioning rotor position due to the armature winding permeance changes. As a result, the magnetic field of the armature winding interacts with excitation sources, turning the electrical energy into mechanical energy for motor operation [3].

---

\*Corresponding author: [erwan@uthm.edu.my](mailto:erwan@uthm.edu.my)

2022 UTHM Publisher. All rights reserved.

[publisher.uthm.edu.my/periodicals/index.php/eeee](http://publisher.uthm.edu.my/periodicals/index.php/eeee)

The issue related to the permanent magnet motor is cogging torque which disturbs the performance of the motor where it also happens on PM-FSM. Cogging torque is produced by the interaction of a permanent magnet that is connected to the stator and the teeth of the rotor due to slotting in the conventional permanent magnet (PM) brushless machines [4]. Cogging torque is caused by the magnetic interaction between the stator permanent magnet and steel laminations of the rotor teeth. In other words, the cogging torque is by the variation of magnetic energy by the rotor angular position [5]. The problem that arises from permanent magnet flux-switching motors (PMFSM) is it produces a higher cogging torque compared to other conventional permanent magnet motors due to their exceptional configuration which is affected by the association between the permanent magnet on stator and rotor teeth. The cogging torque in the motor causes vibration, noise, and deterioration of motor performance [6]. The acceptable amount of cogging torque is 10% was discovered from previous research [7].

So, there are three objectives of this study which is the first is to analyze the performance of Permanent Magnet Flux Switching Motor (PM-FSM) in terms of flux linkage, cogging torque and back emf. The next objective is to decrease the cogging torque of Permanent Magnet Flux Switching Motor (PMFSM) by using three classic techniques which are notching, chamfering and pole pairing techniques. The last objective is to analyze the cogging torque of 4S-8P PM-FSM by introducing a sequential cogging torque reduction technique. The design for 4S-8P PM-FSM will undergo reduction technique of cogging were carried out 2D-FEA solver in JMAG-Designer where it has three technique which notching, chamfering and pole pairing and will influence the geometrical design on the rotor.

## 2. Methodology

The methodology of this study was carried out using J-MAG Designer to design a 4 slot and 8 poles of permanent magnet flux switching motor (PM-FSM) to investigate the performance of cogging torque reduction in 2D finite element analysis (FEA).

### 2.1 Design and Analysis Performance

A complete diagram of 4 slots and 8 poles of PFSM was sketched in Geometry editor by drawing the rotor, stator, permanent magnet, and armature coil part by region mirror pattern and region radial pattern. After completing the drawing, the design is linked with JMAG designer where in this part, the material and condition is implemented to the motor. Figure 1 shows the process flow of sketching the 4S-8P of PM-FSM in JMAG designer.

Next, the first objective this study can be achieved by conducting the no-load analysis after designing 4S-8P PMFSM where the cogging torque, flux linkage and back-emf is analyzed. No-load analysis condition is a condition where there is no current is applied on winding and the voltage is applied. After that, the load analysis is applied to the motor where the armature current is set at  $5A_{rms}/mm^2$  until  $30 A_{rms}/mm^2$  to analyze the effect of armature current to the torque of the motor. Figure 2 shows the flow of performance analysis of 4S-8P PMFSM.

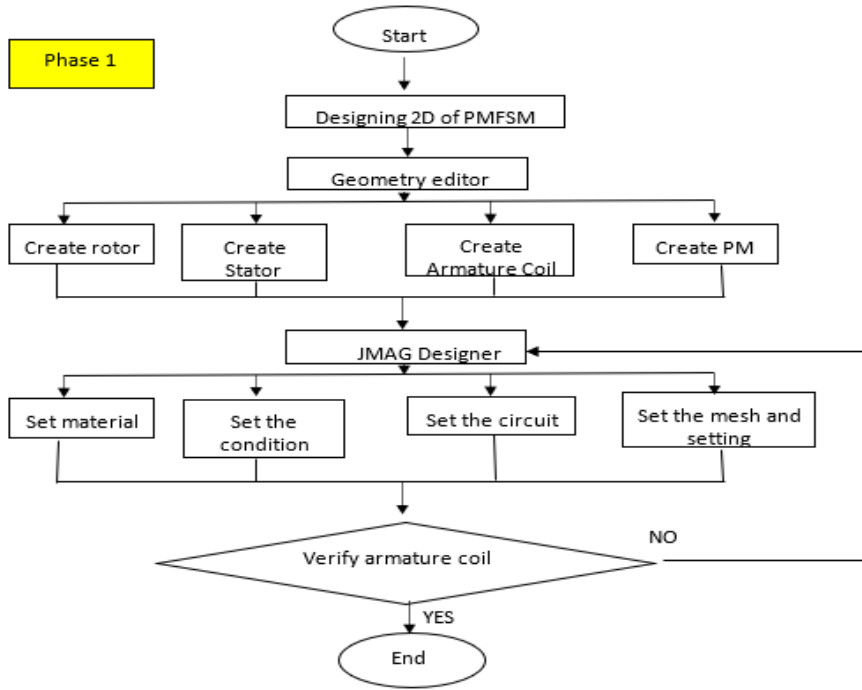


Figure 1: Process of Designing the 4S-8P of PM-FSM

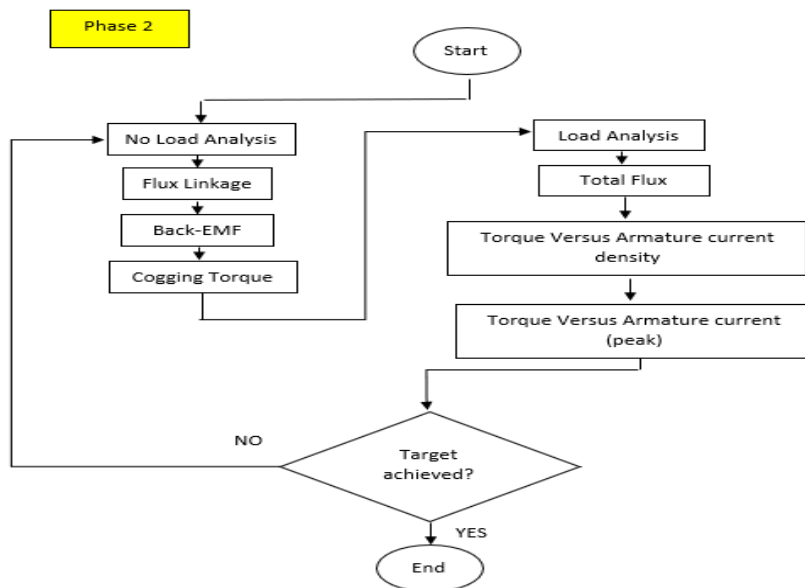


Figure 2: Flow of Performance Analysis of 4S-8P PMFSM

2.2 Cogging Torque Characteristics

The cogging torque is known as the derivative of output torque defined by the Fourier series through the finite element method. The output torque is obtained from the product of the differentials of energy against time as illustrated in Eq. 1

$$P_m = \frac{dW_m}{dt} = T \frac{d\theta}{dt} = Tw \tag{Eq. 1}$$

where  $P_m$  is the power,  $dW_m$  is the product of energy differential,  $d\theta$  is the differential mechanical angle,  $w$  is the angular velocity, and  $T$  is the output torque. Eq. 2 expressed the motor’s torque that is made up of reluctance torque, alignment torque, and cogging torque.

$$T = T_R + T_A + T_{cog} \quad Eq. 2$$

$$T_R = \frac{1}{2} i^2 \frac{dL}{d\theta} \quad Eq. 3$$

$$T_A = Ni \frac{d\phi_g}{d\theta} \quad Eq. 4$$

$$T_{cog} = -\frac{1}{2} (\phi_g)^2 \frac{dR}{d\theta} \quad Eq. 5$$

In Equation 2,  $T$  is torque,  $T_R$  is reluctance torque and  $T_{cog}$  is cogging torque. Following that, the derivation of  $T_R$ ,  $T_A$  and  $T_{cog}$  yields in  $\phi_g$ , air gap flux,  $dR$  is the air gap reluctance and  $d\theta$  is the rotor position. The existence of cogging torque can demonstrate by the interaction of the magnet producing air gap flux between the stator and the rotor in a variable with the air gap reluctance with time, as indicated by the derivation.

The corresponding EMF harmonics of the magnets and the stator magnetic conductance are contributed from periodic changes in the cogging torque caused by periodic changes in the air gap reluctance. The periodical changes in the cogging torque can be evaluated with the Fourier series expressed in (6).

$$T_{cog}(\theta_m) = \sum_{n=1}^{\infty} T_n \sin(kN_e\theta_m + \theta_n) \quad Eq. 6$$

where  $\theta_m$  is the rotor angular position,  $T_n$  is the amplitude of the n-th harmonic,  $\theta_n$  is the phase angle of the n-th harmonic, and  $N_e$  is the smallest common multiple of rotor pole and stator pole.

### 2.3 Sequential Cogging Torque Reduction Technique Performance

From the successful design at the design stage where the torque and current are obtained, then the design will undergo the cogging torque reduction technique to refine the cogging torque of PMFSM to fulfill the objective of reducing the cogging torque of PM-FSM through sequential technique.

The process of sequential cogging torque reduction technique starts with the initial design that will go with three respective classical cogging torque techniques individually which are notching, chamfering and pole pairing which is shown in Figure 3 until Figure 5.

After the motor is applied are implement individual cogging torque technique, the cogging torque variables are identified. The variables are chosen from the lowest cogging torque produced in each technique without factoring in the output power and output torque of the motor in the selection.

Figure 3 until Figure 5 shows the cogging torque reduction is applied individually on a motor. Each technique has different variations such as for notching is the number of notch and notch height. For chamfering are fillet chamfer, right angle chamfer and left angle chamfer. Lastly, for pole pairing, the variable is even pole and odd pole. Based on these variables, the 4S-8P PMFSM was analysed if the value obtained is less than an initial value which is 1.7722Nm, it will value will be used for the sequential technique. If not, the process will go back to the variables of the technique.

The sequential cogging torque techniques for 6 sequence is explained in Figure 6 after identifying the lowest value for three respective classical cogging torque techniques individually which are notching, chamfering, and pole pairing. The sequential cogging torque reduction technique for Sequence A started by implementing notching on the design followed by chamfering and ending with pole-pairing. Then it will go to the next sequence which is Sequence B.

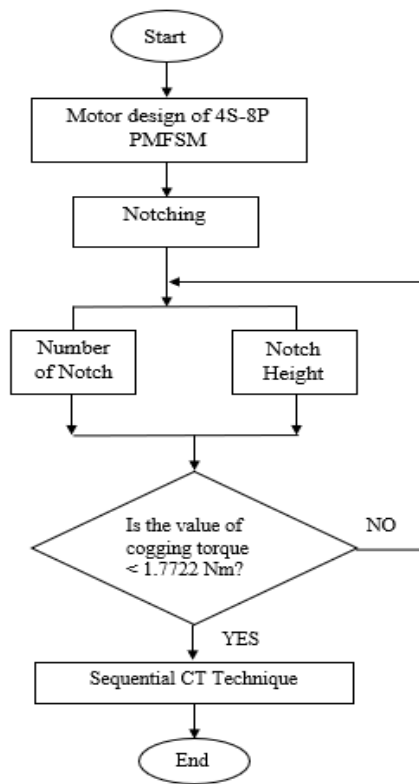


Figure 3: Process flow of notching technique

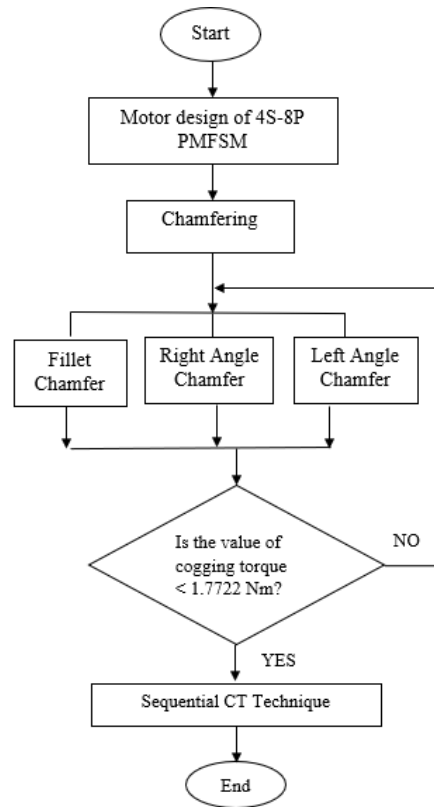


Figure 4: Process flow of chamfering technique

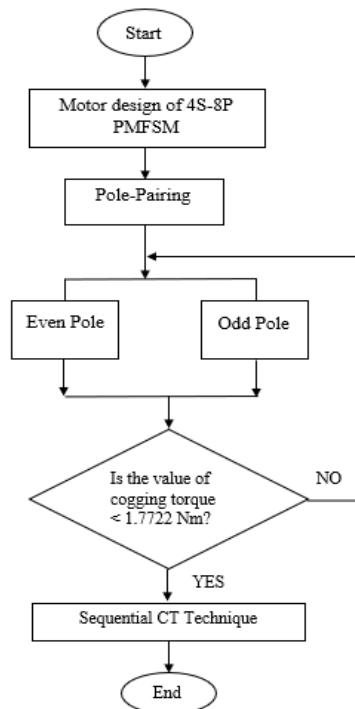
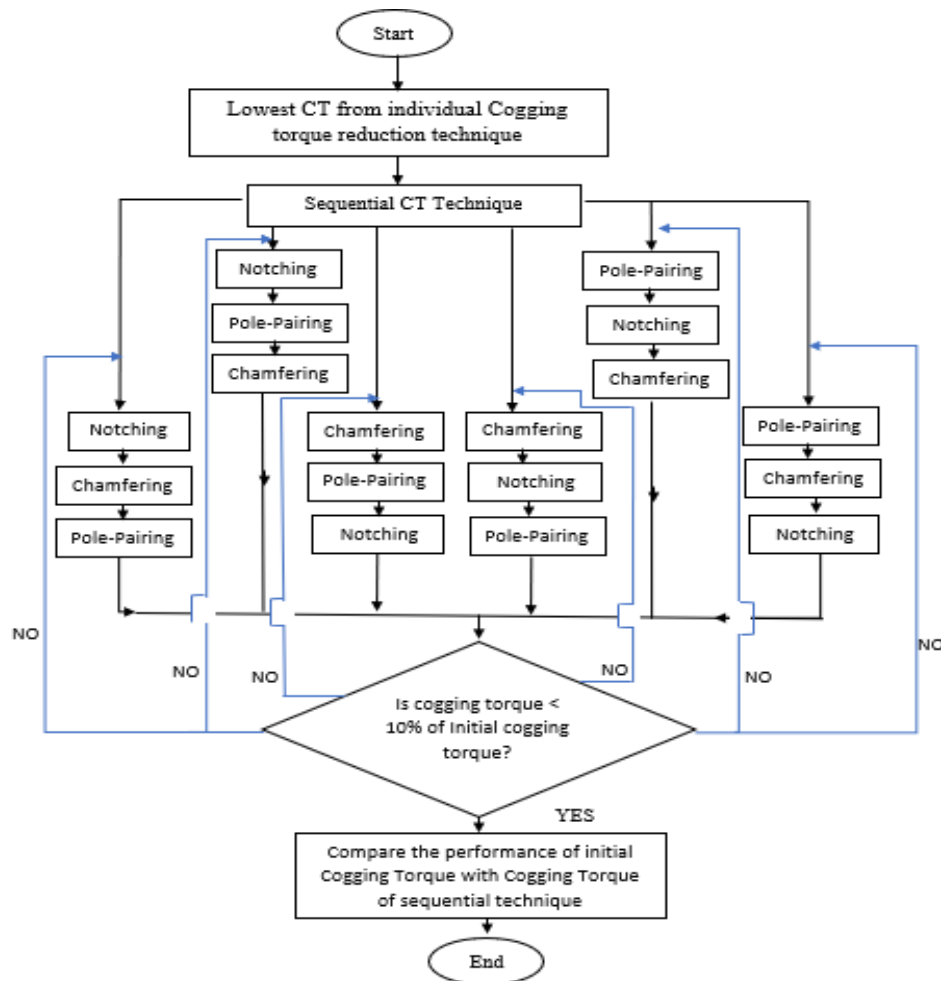


Figure 5: Process flow of pole pairing technique



**Figure 6: Sequential cogging torque reduction technique process flow**

The result from each subsequent technique is individually different as there is no absolute technique. From the result, the design with the variables producing the cogging torque less than 10% of the output torque is chosen. If not, it will go back to the

After that, the initial result of cogging torque is compared with the design that undergoes sequential cogging torque reduction technique to prove these three classical cogging torque techniques can reduce the cogging torque performance of the motor.

### 3. Results and Discussion

The result and analyses of the PMFSM are carried out using 2D-FEA are presented. The first part of the analysis is associated with the first objective which is to analyze the performance of flux linkage, cogging torque, and back emf by designing a 4S-8P PMFSM and the result is recorded as the initial design. Next, the result to minimize the performance of cogging torque for PMFSM using classical cogging torque reduction techniques is conducted. Then, the result of cogging torque reduction is discussed using the sequential cogging torque reduction technique where the performance of 4S-8P PMFSM is evaluated based on the percentage of the cogging torque being reduced.

### 3.1 Performance Analysis Based on 2D Finite Element Analysis

The performance correlation is achieved for 4S-8P of PMFSM with no-load analysis. For no load analysis, the  $J_a$  is set at  $0 \text{ A/mm}^2$  to analyses the performance of the flux linkage, cogging torque and back emf.

#### 3.1.1 Flux linkage Analysis

By rotating the rotor at speed of 1200 r/min while the armature current is set at  $0 \text{ A/mm}^2$ , the amplitude of PM generated magnetic flux linkage for initial design is achieved. The maximum value of the flux is 0.113 Wb and the flux linkage of 4S-8P for PMFSM design is illustrate in Figure 7. The flux leakage and cancellation which take place in the rotor produce the high amplitude of flux linkage, which has an impact on the magnitude of the flux link.

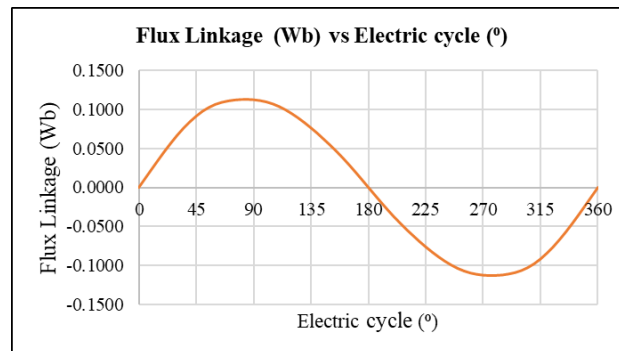


**Figure 7: Flux Linkage Analysis Performances**

#### 3.1.2 Cogging Torque Analysis

Cogging torque is known as unwanted torque or it is called detent torque which produces vibration and noise during the operation of the motor. This is because of the interaction of a permanent magnet in the stator and the mechanical angular position of the rotor. The cogging is delivered by a permanent magnet for one electrical cycle by setting the armature current density,  $J_a$  at  $0 \text{ A/mm}^2$ . The result of cogging torque obtained from the JMAG software in Figure 8 shows the maximum and minimum value of cogging torque which is 0.8893 Nm and -0.8830 Nm and the value of cogging torque of the motor design is determined by peak-peak value which is 1.7722 Nm and the cogging torque in 4S-8P of PMFSM can be refined by using the cogging torque reduction technique.

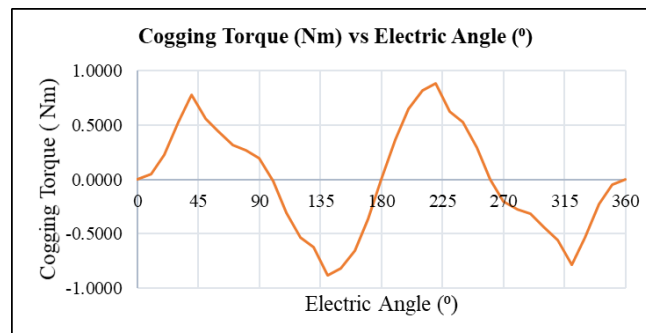


**Figure 8: Cogging Torque Analysis Performance**

#### 3.1.3 Back EMF Analysis

At an open circuit, the analysis of induced voltage can be defined as the voltage that rises in electric motors when there is relative movement between the motor armature and the magnetic field of the motor field magnets, or windings which are known as back electromagnetic force (EMF) can be defined when

the armature current density,  $J_a$  at  $0 A/mm^2$ . The waveform of back-emf for PMFSM is shown in Figure 9. The highest amplitude value for 4S-8P PMFSM is 134.87V and the lowest amplitude value is -112.41V. The rotor pole is located near the stator pole, it has caused ore flux lines to be dispersed throughout the rotor and stator pole. As a result of the more aligned flux lines, there was less back EMF.

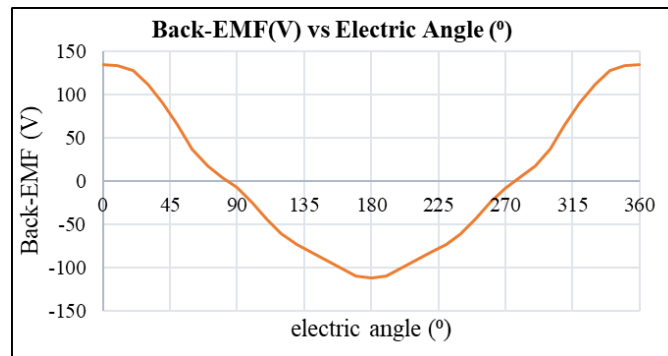


**Figure 9: Back-EMF Analysis Performance 3.2 Discussions**

### 3.2 Performance of Classical Cogging Torque Reduction Technique

#### 3.2.1 Notching

The influence of parameters for notching technique has been investigated with 2D-FEA such as the number of notch and notch height on the initial design of cogging torque of 4S-8P PMFSM is recorded which is shown in Figure 10. The total number of notches that are being investigated is 6th notch. Based on Figure 10 demonstrates that when the number of notch increases, the cogging torque decreases from its initial value of 1.7722Nm of peak-to-peak cogging torque. The lowest cogging torque is recorded when the notch is at the 5th notch which is 1.2007 Nm.

Throughout this research, a study of factors that influence the cogging torque was carried out by varying the height of the notch while width is kept constant. The notch height has been investigated from 0.5mm to 2mm while the width of the notch is fixed at 0.5mm. The FEA was conducted against various notch heights. The value of peak-to-peak cogging torque is decreased dramatically as the notch height increased until the 5th notch is shown in Figure 11. At the 6th notch, the cogging torque is increased when the height notch is increased. To explain the decline in cogging torque due to the variance factor. With increasing the number of notches and notch height, the variation amplitude and periods decreased, lowering the peak-to-peak value of cogging torque.

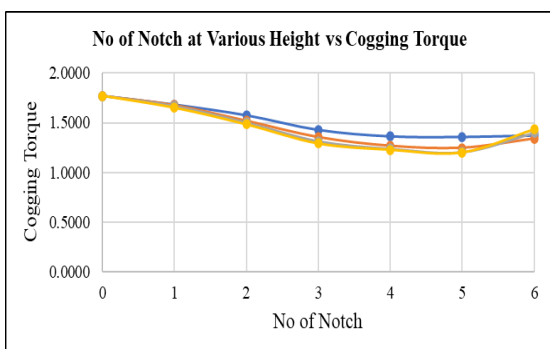


**Figure 10: Influence of the notch number on cogging torque of 4S-8P PMFSM topology**

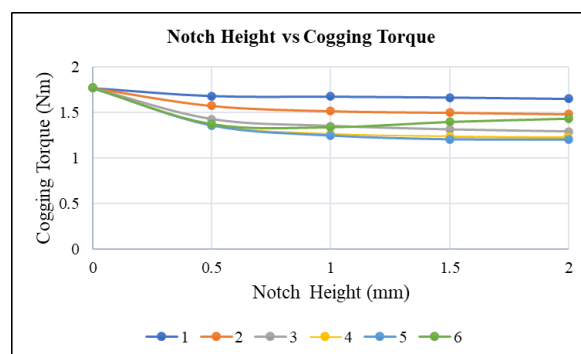


**Figure 11: Influence of the notch height on cogging torque of 4S-8P PMFSM topology**

### 3.2.2 Chamfering

The width and height of the angle cut on the rotor's tip set the dimensions for all chamfers. The dimension of the chamfer is measured when the height and width parameter is at 0.1mm until 0.5mm on angle cut on the tip of the rotor. For right-angle chamfer, the chamfer dimension is investigated at the right-angle cut at the tip of the rotor. The same routine is also applied to the left-angle chamfer. But for fillet chamfer is applied where the fillet cut of the rotor tip is employed on both tips of all rotor poles.

The cogging torque is decreased when the height and width are at 0.1mm. When the height and width are above 0.1mm, the cogging torque is increased when the parameter is increased. Figure 12 demonstrated the effect of chamfering on cogging torque. The right-angle chamfer is recorded as the lowest value of peak-to-peak cogging torque which is from 1.1192Nm to 1.1068Nm compared with other types of chamfer techniques.

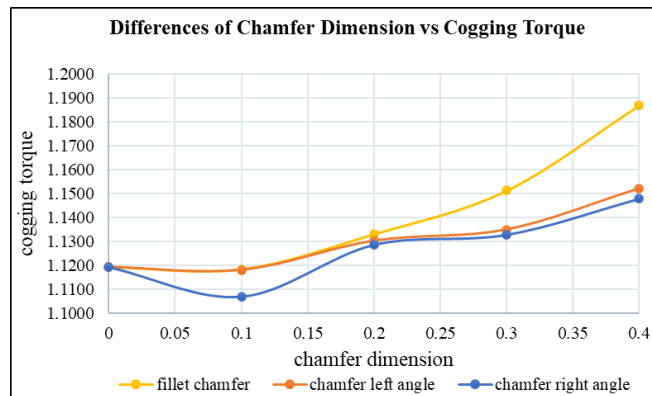


Figure 12: The cogging torque against different of chamfer dimensions

### 3.2.3 Pole Pairing

One of the classical cogging torque reduction techniques which involve geometrically coupling two different angles of rotor poles is known as pole pairing. This technique is applied on the rotor of 4S-8P PMFSM by manipulating the angle of one pole while the other pole remains constant.

The first manipulative pole that is marked as unknown X is defined as an even pole while the unknown Y for the second pole will be defined as an odd pole. The analysis of cogging torque after the first cycle is obtained with FEA. The result of the cogging torque is investigated by manipulating the angle from its original position. The angle for the first pole that is marked as unknown X will shift from their original position with the range  $\pm 5^\circ$  while the angle second pole marked as unknown Y remains constant. The step is repeated by reversing the pole where the second pole marked as unknown Y will be manipulative pole while the first pole marked as unknown X will be fixed their angle.

Figure 13 shows the influence of pole pairing technique cogging torque. Based on the graph above, both cycles show an increment and decrement of cogging torque. For lowest cogging torque recorded for the even pole is 1.4568Nm when the pole is at  $-2^\circ$  while for the odd pole, the lowest cogging torque when the pole is at angle  $47^\circ$  which is 1.4385Nm.

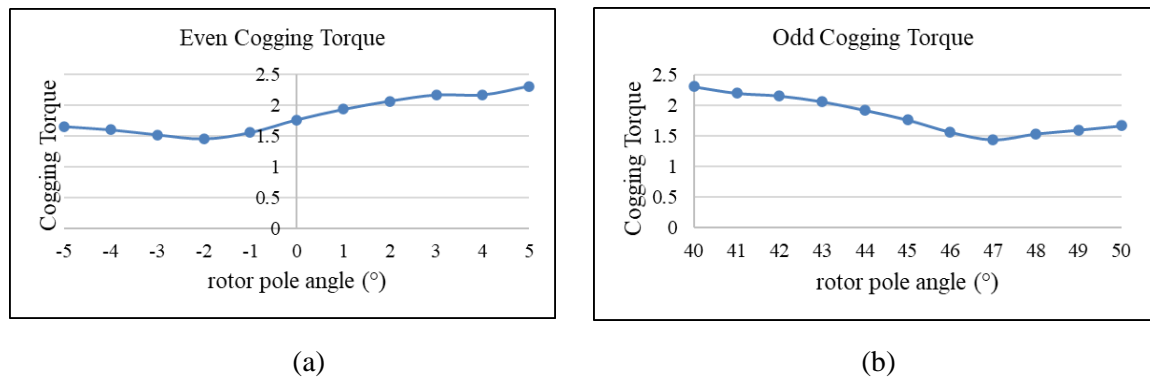


**Figure 13: The effect of even and odd pole against cogging torque**

### 3.3 Performance of Sequential Cogging Torque Reduction Technique.

The sequential cogging torque reduction technique is created to discover the minimal cogging torque possible. The acceptable amount of cogging torque is 10% was discovered from previous research [7]. Table 1 explained in more detail the percentage of cogging torque reduction based on the previous parameter for three classical cogging torque reduction techniques. For notching technique, the parameter that is used for sequential technique is when the notch is at 5th and the height is 2mm, while for chamfering, the height and width for all chamfering dimension is at 0.1mm. Last but not least, the lowest cogging torque during individual analysis show for even pole, the angle is at  $-2^\circ$  while for odd pole is at  $47^\circ$ .

Figure 14 shows the comparison of initial cogging torque and the cogging torque that undergoes sequential cogging torque reduction technique. The lowest cogging torque recorded based on the sequence is sequence A and sequence F which is 37.28% from the initial cogging torque value.

**Table 1: The Cogging Torque and Percentage Reduction of Cogging Torque**

No	Sequential Cogging Torque Reduction Component				Cogging Torque	% Reduction of CT
1	NON	NH	LFC	EP	1.1116	37.28
2	NON	NH	EP	LFC	1.1166	36.99
3	LFC	EP	NON	NH	1.1139	37.15
4	LFC	NON	NH	EP	1.1182	36.90
5	EP	NON	NH	LFC	1.1125	37.22
6	EP	LFC	NON	NH	1.1116	37.28

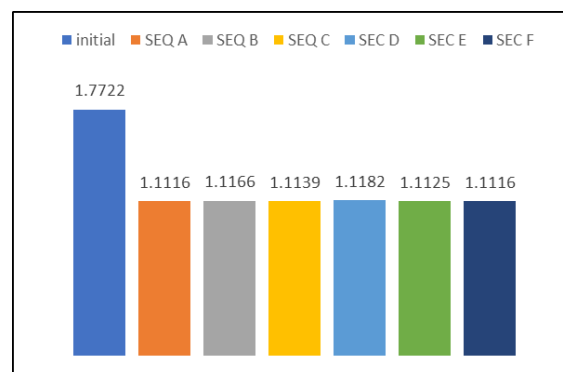


**Figure 14: The comparison of initial cogging torque with a cogging torque that undergoes sequential cogging torque reduction**

#### 4. Conclusion

In conclusion, this research objective on single-phase motor of PMFSM has been obtained successfully. The 4S-8P PMFSM is designed using JMAG Designer by designing the rotor, stator, armature coil, and a permanent magnet. For the first objective which is to analyze performance of flux linkage, cogging torque, and back emf on the motor has been completed during no-load analysis which used as initial reading to achieve the second objective.

Next, the classical individual cogging torque technique, such as chamfering, notching and the pole pairing technique has been successfully conducted on 4S-8P PMFSM as second objective. It was recorded that for notching technique, the 5<sup>th</sup> notch is the lowest peak to peak value of cogging torque. For chamfering technique show result that right-angle chamfer has lower cogging torque value compare to another chamfer. Lastly, for pole pairing technique is an odd pole where the angle at 47°.

The third objective of improving and analyzing the cogging torque performance by using cogging torque reduction technique in sequential has been utilized to the initial design. The cogging torque is minimized as much as 35% from the targeted value which is 10% from the initial peak-to-peak cogging torque.

#### Acknowledgement

The authors would like to thank the Faculty of Electrical and Electronic Engineering, Universiti Tun Hussein Onn Malaysia for its support.

#### References

- [1] Y. Wang, J. Shen, Z. Fang, and W. Fei, "Reduction of Cogging Torque in Permanent Magnet Flux-Switching Machines," *J. Electromagn. Anal. Appl.*, vol. 01, no. 01, pp. 11–14, 2009, doi: 10.4236/jemaa.2009.11003.
- [2] Y. Zhou, L. Zhou, B. Hu, and R. Li, "Design and performance analysis of permanent magnet flux-switching motors using segmental permanent magnets," *IEICE Electron. Express*, vol. 16, no. 11, pp. 1–6, 2019, doi: 10.1587/elex.16.20190193.
- [3] E. I. Mbadiwe and E. Bin Sulaiman, "Design and optimization of outer-rotor permanent magnet flux switching motor using transverse segmental rotor shape for automotive applications," *Ain Shams Eng. J.*, vol. 12, no. 1, pp. 507–516, 2021, doi: 10.1016/j.asej.2020.08.007.
- [4] Z. Q. Zhu, A. S. Thomas, J. T. Chen, and G. W. Jewell, "Cogging Torque in Flux-Switching Permanent Magnet Machines," *IEEE Trans. Magn.*, vol. 45, no. 10, pp. 4708–4711, 2009, doi: 10.1109/TMAG.2009.2022050.
- [5] J. X. Shen and W. Z. Fei, "Permanent magnet flux switching machines - Topologies, analysis and optimization," *Int. Conf. Power Eng. Energy Electr. Drives*, no. February 2017, pp. 352–366, 2013, doi: 10.1109/PowerEng.2013.6635633.
- [6] Y. Wang, M. J. Jin, W. Z. Fei, and J. X. Shen, "Cogging torque reduction in permanent magnet flux-switching machines by rotor teeth axial pairing," *IET Electr. Power Appl.*, vol. 4, no. 7, pp. 500–506, 2010, doi: 10.1049/iet-epa.2009.0205.
- [7] S. N. U. Zakaria and E. Sulaiman, "Performance analysis of E-Core hybrid excitation flux switching motor for hybrid electric vehicle," *Proc. 2014 IEEE 8th Int. Power Eng. Optim. Conf. PEOCO 2014*, no. March, pp. 318–323, 2014, doi: 10.1109/PEOCO.2014.6814447.